

Supporting information for “Quasi-3D Gold Nanoring Cavity Arrays with High-Density Hot-Spots for SERS Applications via Nanosphere Lithography”

Chi-Chih Ho^{a,c}, Ke Zhao^b and Tze-Yang Lee^{a}*

a) Department of Engineering and System science, National Tsing Hua University, Hsinchu, Taiwan.

b) Department of Physics and Astronomy, and Laboratory for Nanophotonics, Rice University, 6100 Main Street, Houston, Texas 77005, United States

c) Taiwan international graduation program, Nanoscience and technology program, Institute of Chemistry, Academia Sinica, Taipei, Taiwan

Section 1: The analytical enhancement factors

For practical use, analytical enhancement factors (AEF) are often considered to evaluate the efficiency of a SERS substrate.^{1,2} A constant volume of R6G solution (V_{R6G}) was dropped on SERS substrates, followed by covering with a glass slide for sealing. The thickness of the liquid (h) between SERS substrate and cover glass is estimated by $h = V_{R6G}/A$, where A is the area of the SERS substrate (about 5mm x 5mm). The illuminating size of laser beam is S_{laser} , see Figure S1(A). The total numbers of R6G molecules within the excitation volume on SERS substrate can be expressed as $N_{SERS} = C_{R6G} \times S_{laser} \times h \times NA$, where C_{R6G} and NA are the concentration of R6G solution (2×10^{-6} M) and Avogadro's number. Therefore, the AEF can be obtained by inserting these values into:

$$AEF = \frac{(I_{SERS}/N_{SERS})}{(I_{RS}/N_{RS})}$$

The I_{SERS} is the intensity of SERS signal measured at Raman shift = 1360 cm^{-1} , which is assigned to the aromatic C-C stretching of R6G molecule. The measurements of ordinary Raman scattering, the I_{RS} , as the reference were carried out using the R6G concentration of $2 \times 10^{-2} \text{ M}$ on a flat gold surface.

For the analysis of SERS data, the measured spectra were further corrected by baseline adjustment. The backgrounds were removed, as illustrated in Fig. S1(B). The background is the spectrum measured simply from deionized water (DIW) on each SERS substrate. The noise level of Raman spectrometer is retained from measuring 15 spectra of DIW on planar gold. The root mean square of noise amplitude is estimated to be $\text{RMS}_{\text{noise}} \sim 50 \text{ (a.u.)}$. The signal to noise ratio is determined by $I_{\text{SERS}}/\text{RMS}_{\text{noise}}$, which ranged from ~ 5 to 140 in this study.

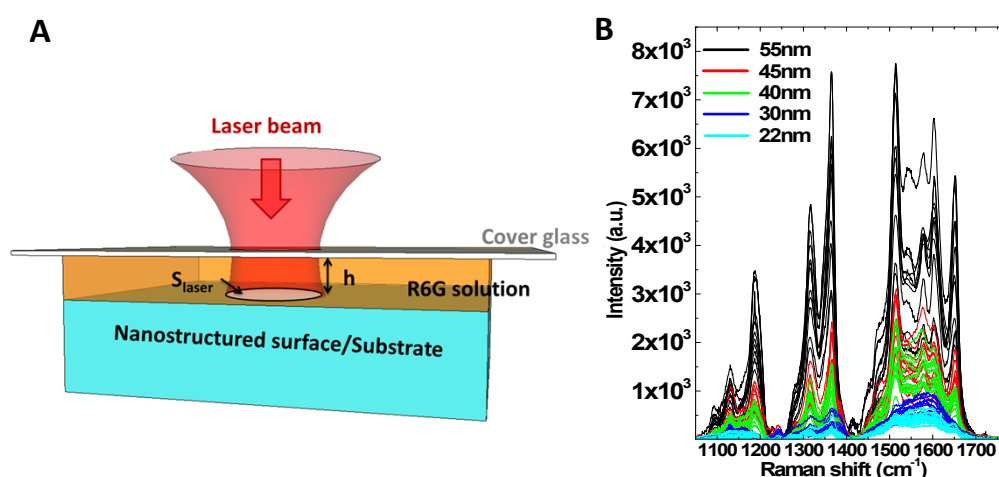


Figure S1. (A) A 3D cartoon illustration of measurement setup. The laser beam is

focused at the surface of substrate with spot of S_{laser} . The R6G solution after covering with glass slide has a thickness h . (B) SERS of R6G measured with respect to the setup in (A). Different colors represent different thickness of gold on nanoring cavity. There were 10-15 patches on each nanoring-cavity-templated substrate measured from a specific thickness of gold.

Section 2: Ordering characterization using a 266 nm laser diffractive method

Macroscopic sample quality was examined by diffraction pattern measurements using a 266 nm laser beam. The spot size of incident laser is estimated to be 2.5 mm in diameter. The sample was mounted on a micro stage with a laser beam incident normal to surface. Backward diffraction beams were captured by a fluorescent screen. Six-fold symmetric diffraction spots became visible and can be recorded by CCD. Diffraction patterns from ten areas on the sample were collected along the sample axis, which gave a polycrystalline feature. The maximum number of crystal orientations is three in our observation. Hence, we suggest the millimeter-sized long-range ordering in the sample.

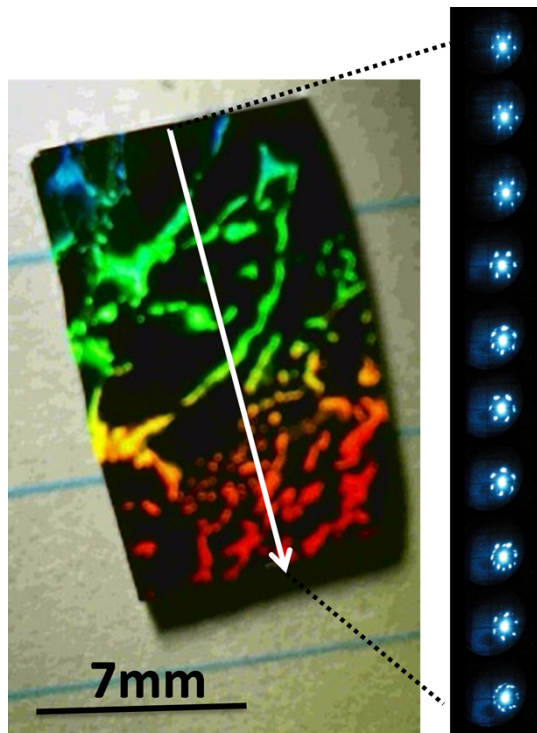


Figure S2 Diffraction patterns of our prepared sample excited from 266 nm laser. The maximum numbers of crystal orientation observed in 2.5 mm laser spot is 3, which means a millimeter-sized ordering in the sample. The white arrow indicates the scanning direction of laser beam. Corresponding diffraction patterns are shown at right side. The colorful pattern on the left side results from the diffraction of white light due to the periodic nanostructure. The uniform diffracted color confirms the same crystal orientation and ordering in the area.

Section 3: Simulation results

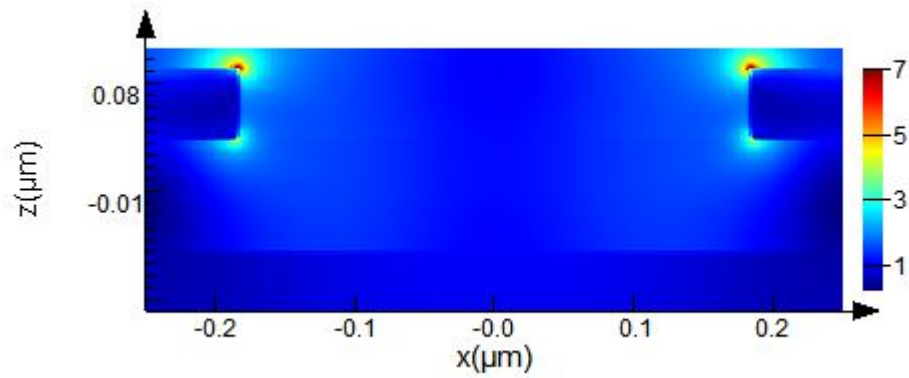


Figure S3.1 Field enhancement distribution E/E_0 of a nanohole with 55 nm gold corresponding to Fig. 5(A) of the manuscript.

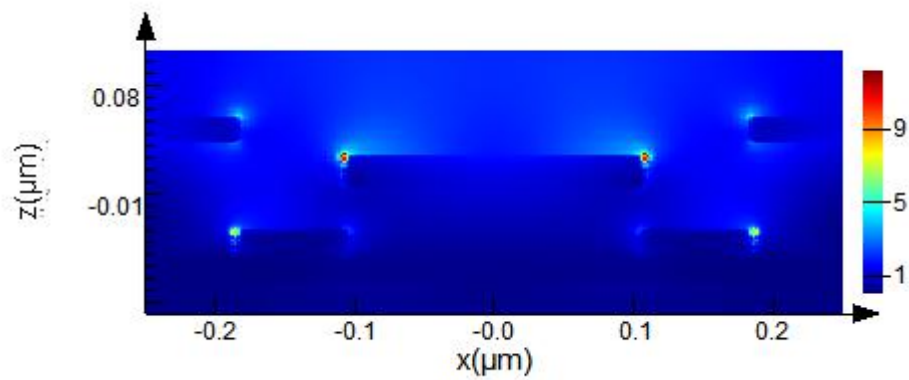


Figure S3.2 Field enhancement distribution E/E_0 of a nanoring cavity with 20 nm gold corresponding to Fig. 6(A) of the manuscript.

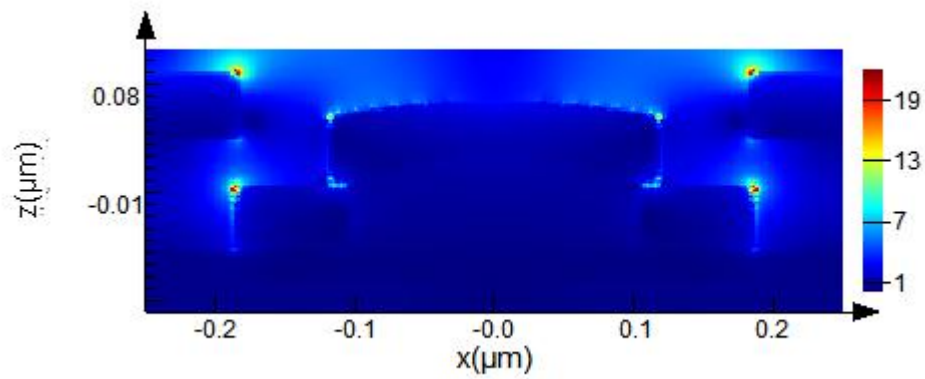


Figure S3.3 Field enhancement distribution E/E_0 of a nanoring cavity with 55 nm gold corresponding to Fig. 6(B) of the manuscript.

Section 4: Measured reflectivity with different gold thickness

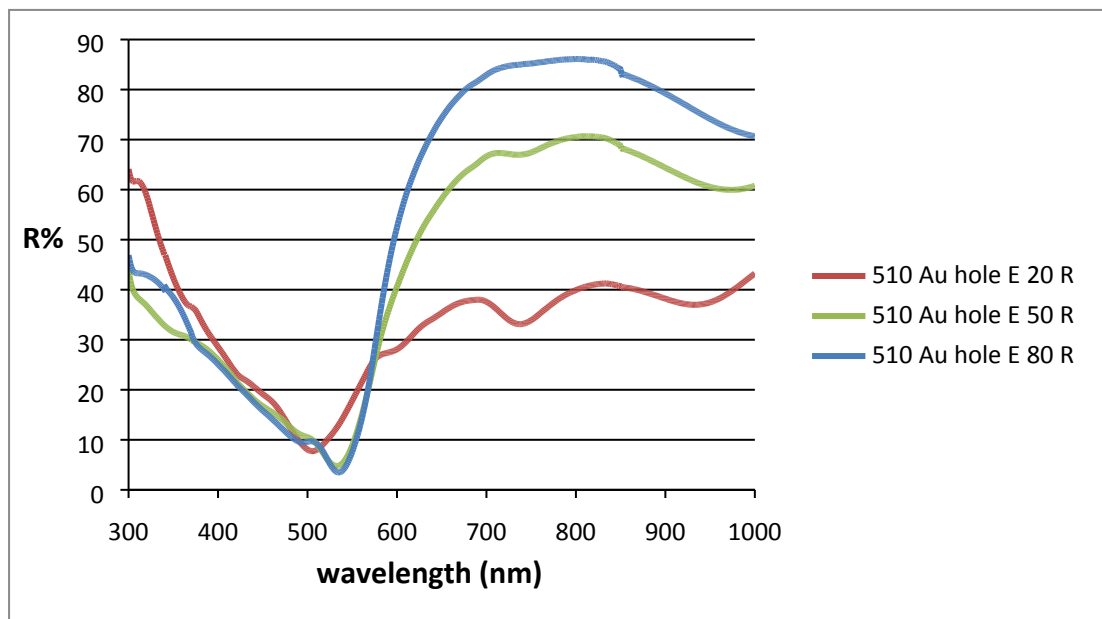


Figure S4.1 Measured reflectivity from nanohole+disc arrays with 20, 50 and 80 nm gold thickness. The period was fixed to 510 nm. The environment for measurements is air.

Section 5: Reflectivity for nanohole array at period of 780nm, gold thickness of 55nm and hole diameter in 645nm.

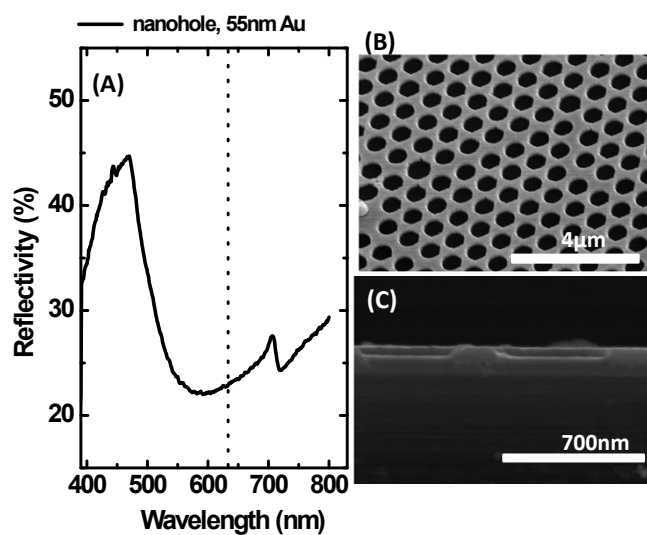


Figure S5 (A) The measured spectrum of nanohole array with period of 780 nm, diameter in 645 nm and gold thickness of 55 nm in deionized water. (B) and (C) are SEM images of top view and cross sectional view.

References

- (1) Le Ru, E. C.; Blackie, E.; Meyer, M.; Etchegoin, P. G. *The Journal of Physical Chemistry C* **2007**, *111*, 13794.
- (2) Bahns, J. T.; Guo, Q.; Montgomery, J. M.; Gray, S. K.; Jaeger, H. M.; Chen, L. *The Journal of Physical Chemistry C* **2009**, *113*, 11190.